

## Dissolution of iron in aluminium alloys

### Raztapljanje železa v aluminijevih zlitinah

STANISLAV KORES<sup>1</sup>, MAJA VONČINA<sup>1</sup>, PRIMOŽ MRVAR<sup>1</sup>, JOŽEF MEDVED<sup>1</sup>

<sup>1</sup>University of Ljubljana, Faculty of Natural Sciences and Engineering,  
Department of Materials and Metallurgy, Aškerčeva cesta 12, SI-1000 Ljubljana, Slovenia;  
E-mail: stanislav.kores@ntf.uni-lj.si, maja.voncina@ntf.uni-lj.si, primoz.mrvar@ntf.uni-lj.si,  
jozef.medved@ntf.uni-lj.si

**Received:** November 6, 2007

**Accepted:** December 20, 2007

**Abstract:** Iron presents in Al-alloys the main impurity, but in some alloys iron presents an alloying element, which increases the hardness of the alloys, but also increases brittleness. In this work the dissolution of iron in electrolytic aluminium and AlSi12Cu(Fe) alloy has been investigated. In experiments iron wire was dissolved in the investigated alloys at temperature 750 °C for 0, 15 and 30 minutes. These specimens were characterized using scanning electron microscope (SEM) and EDS analyzer, in order to determine concentration of iron in the aluminium and to identify iron phases. With the simultaneous thermal analysis (STA) the characteristic temperatures and the solidification, melting and precipitation heats of investigated alloys with dissolved iron were determined. Using the Thermo-Calc simulation program the equilibrium phases were calculated, special emphasis was given to iron phases that form during solidification.

**Izvleček:** Železo predstavlja v aluminijevih zlitinah glavno nečistočo, pri nekaterih zlitinah pa predstavlja zlitinski element, ki povečuje trdoto zlitine in krhkost zlitine. V tem delu se je preiskovalo raztapljanje železa v elektroliznem aluminiju in zlitini AlSi12Cu(Fe). Eksperimentalno je bilo raztapljanje železa opazovano z raztapljanjem železove žičke pri temperaturi 750 °C in času 0, 15 in 30 minut. Vzorci so bili preiskani z vrstičnim elektronskim mikroskopom (SEM) in EDS analizatorjem za določitev koncentracije železa v aluminiju in za definiranje železovih faz. Z uporabo simultane termične analize (STA) so bile definirane karakteristične temperature strjevanja in taljenja ter latentne toplote izločanja preiskovanih zlitin z raztopljenim železom. Z računalniško simulacijo Thermo-Calc so bile izračunane ravnotežne faze, predvsem železove faze, ki se tvorijo pri strjevanju.

**Key words:** Al-alloys, iron dissolution, thermal analysis, thermodynamic equilibrium

**Ključne besede:** aluminijeve zlitine, raztapljanje železa, termična analiza, termodinamično ravnotežje

## INTRODUCTION

Iron presents in Al-alloys the main impurity that aggravates ductility and corrosion behaviour. Iron in aluminium is gained from ore, from master alloy or from tools that are used during melting and aluminium casting. Another source of iron in aluminium can be scrap of metallurgical aluminium. In some alloys iron is added as an alloying element to increase hardness; however it also increases the brittleness of the alloys as a side effect. The aim of this work was to determine the dissolution of iron in electrolytic aluminium and AlSi12Cu(Fe) alloy with 0.8 wt.% of Fe. Experiments were carried out in an electrical-resistance furnace at 750 °C. The iron wire was placed into the melt and stayed in it at this temperature over different times. After the preset time the furnace was

turned off and samples were cooled down to the room temperature. Samples were investigated using a scanning electron microscope (SEM), an EDS analyzer and simultaneous thermal analysis (STA). Equilibrium solidification was calculated by the Thermo-Calc simulation program.

## INFLUENCE OF IRON CONCENTRATION IN AL-ALLOYS ON SOLIDIFICATION PROCESS

For the study of aluminium alloys, where iron is the main alloying element the equilibrium phase diagram Al-Fe, which is presented in Figure 1 was used<sup>[1]</sup>. Solubility of iron in solid aluminium is very low and amounts 0.04 wt.% at 625 °C<sup>[1]</sup>.

When concentration of iron exceeds 10 wt.% in the system Al-Fe, a peritectic

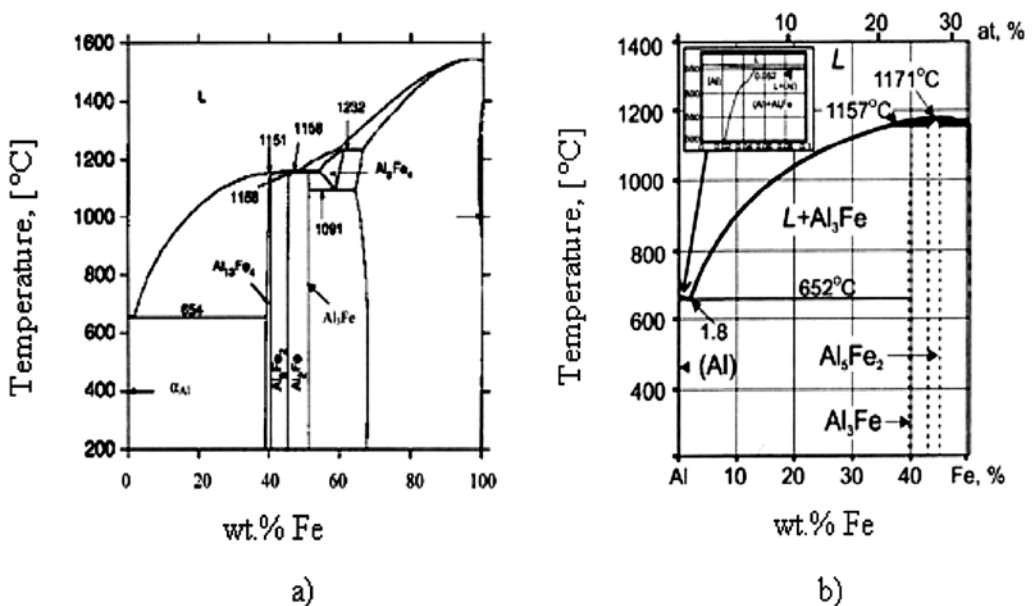


Figure 1. Equilibrium phase diagram Al-Fe (a) and the aluminium-rich corner (b)<sup>[1]</sup>  
Slika 1. Ravnotežni fazni diagram Al-Fe (a) in njegov aluminijev kot (b)<sup>[1]</sup>

reaction  $L + Al_5Fe_2 \rightarrow Al_3Fe$  takes places at temperature 1158 °C, which causes formation of  $Al_3Fe$  phase, which contain 40.7 wt.% Fe (Figure 1). This phase appears in microstructure in the form of needlelike crystals and is fragile and unwished<sup>[1]</sup>.

In Al-Si casting alloys in addition to  $\beta-Al_5FeSi$  phase numerous other phases

can be present<sup>[2]</sup>. In Figure 2 the aluminium corner of ternary phase system Al-Fe-Si is presented<sup>[3]</sup>.

Depending on chemical composition and solidification conditions in microstructure of Al-Si casting alloys the following intermetallic phases could be observed:  $\alpha-Al_8Fe_2Si$ ,  $\beta-Al_5FeSi$  and  $\delta-Al_9FeSi_3$  as

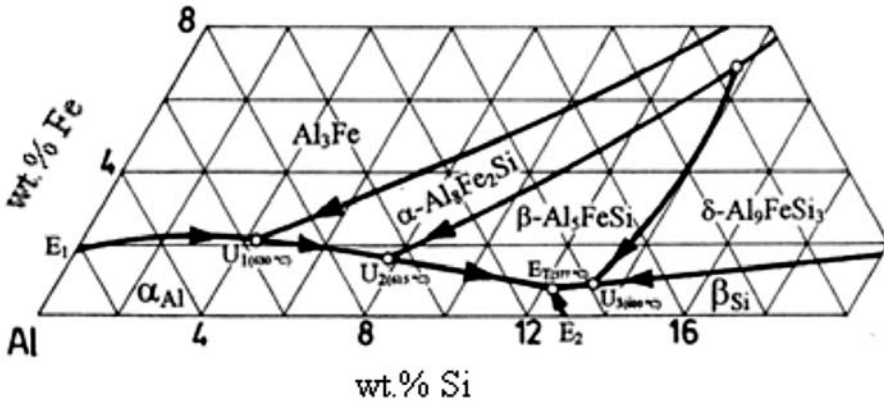


**Figure 2.** The aluminium corner of the ternary system Al-Fe-Si <sup>[3]</sup>  
**Slika 2.** Aluminijev kot ternarnega sistema Al-Fe-Si <sup>[3]</sup>

**Table 1.** Binary and multi-component phases containing iron in Al-Si cast alloys<sup>[2]</sup>  
**Tabela 1.** Binarne in večkomponentne spojine z železom v Al-Si zlitinah<sup>[2]</sup>

Phase	Chemical composition (wt.%)
$Al_{13}Fe_4$ ( $Al_3Fe$ )	Fe: 33.9-37.8; Si: 0.8-2.9
$Al_6Fe$	Fe: 25.6-28.0
$\beta-Al_5FeSi$	Fe: 23.5-30.0; Si 12.0-18.9
$\beta-Al_{4.5}FeSi$ ( $Al_9Fe_2Si_2$ )	Fe: 27.0-28.0; Si 14.0-15.0
$\gamma-Al_3FeSi$	Fe: 33.0-38.0, Si: 13.0-18.5
$\delta-Al_9FeSi_3$	Fe: 15.0-25.4; Si: 20.0-25.5
$\alpha-Al_8Fe_2Si$	Fe: 28.2-31.6; Si: 7.9-10.5
$Al_9Fe_{0.84}Mn_{2.716}Si$	Fe: 10.7; Si: 6.44; Mn: 27.2
$\pi-Al_8Si_6Mg_3Fe$	Fe: 8.0; Si: 25.0-33.8; Mg: 13.0-16.0
$\alpha-Al_{12-15}(Fe,Mn,Me)_3Si_{1-2}$ , Me=(Cr,Cu)	Fe: 8.6-30.7; Si: 4.5-12.5; Mn: 0.52-14.0; Cu: from 7.5, Cr: to 14.4
$\alpha-Al_{12-25}(Fe,Me)_{2-3}Si_{2-4}$ , Me=(Mn,Cr,Cu,Co,Ni)	Fe: 6.3-25.2; Si: 4.6-10.0; Mn: to 13.1; Cu: to 13.0, Cr: to 14.4; Co: to 20.1; Ni: to 26.8
$Al_{19}Fe_4MnSi_2$	Fe: 19.2; Si: 8.3; Mn: 7.8; Cu:2.5; Cr: 0.2

primary crystallized phases. Most often precipitated phase in Al-Si casting alloys is  $\beta$ -Al<sub>3</sub>FeSi phase. Table 1 shows typical binary and multi-component phases with iron and other alloying elements in Al-Si castings alloys.

## EXPERIMENTAL WORK

Iron dissolution was investigated in molten electrolytic aluminium and AlSi12Cu(Fe) alloy. Chemical compositions of investigated alloys are shown in Table 2.

Samples were melted in an electrical-resistance furnace in a graphite crucible. When the temperature of the melt reached 750 °C, iron wire was placed into the melt in the middle of the crucible (Figure 3). Dissolution of iron wire was observed at temperature 750 °C for 0 min, 15 min in 30 min. After these preset times the furnace was turned off. The cooling was continued down to the room temperature.

The samples were cut into two halves next to the iron wire (Figure 4). The samples were investigated using a scanning

**Table 2.** Chemical composition of investigated alloys in wt.%

**Tabela 2.** Kemijska sestava preiskovanih zlitin v mas.%

	SI	FE	CU	MN	MG	ZN	TI	AL
Electrolytic Al	0.041	0.1497	<0.0008	<0.0001	0.0011	0.0089	0.0001	rest
AlSi12Cu(Fe) alloy	11.5584	0.8292	0.7159	0.1915	0.0546	0.4673	0.0466	rest

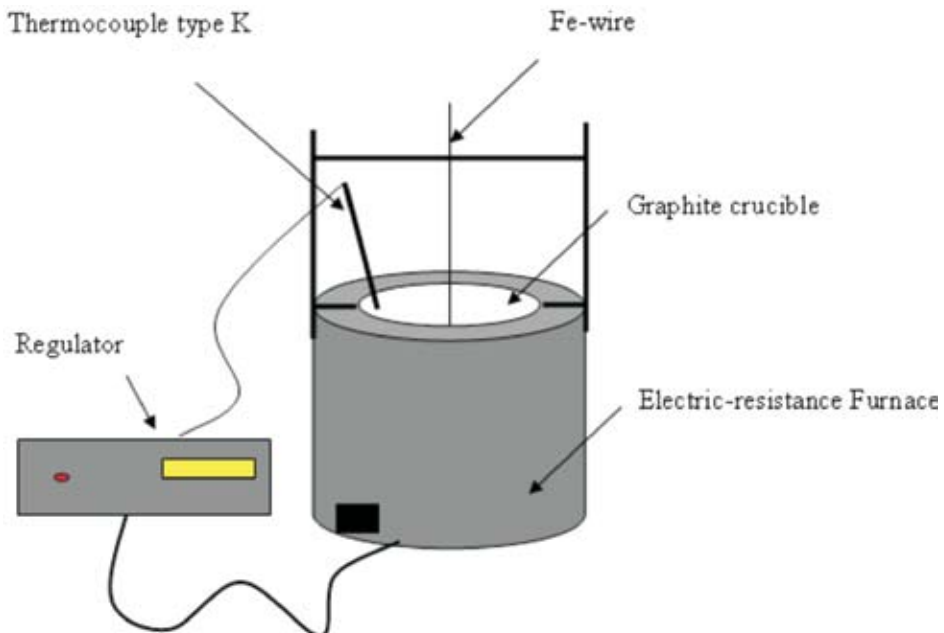


**Figure 3.** Scheme of the experimental set-up  
**Slika 3.** Shema eksperimentalne naprave

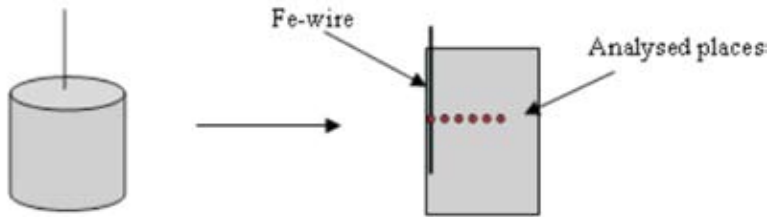


**Figure 4.** Scheme of a cut sample and analysed places

**Slika 4.** Shema razreza vzorca s prikazanimi analiziranimi mesti

electron microscope (SEM) JEOL JSM-5610. They were prepared by the standard metallographic procedure. The samples were analysed at sites shown in Figure 4. On the basis of iron analysis in Al and AlSi12Cu(Fe) a diagram, iron concentration versus distance from the iron wire was constructed.

AlSi12Cu(Fe) samples were researched with simultaneous thermal analysis (STA) on the STA 449 NETZSCH apparatus. The specimens were heated to 720 °C with heating rate of 10 K/min in an argon protective atmosphere and cooled with the same rate down to the room temperature.

With computer simulation Thermo-Calc were defined existence of thermodynamic equilibrium phases in electrolytic aluminium and AlSi12Cu(Fe) alloy with 0.8 wt.% Fe. The aim was to determine which iron phases may form during solidification.

## RESULTS AND DISCUSSION

Using computer simulation Thermo-Calc the existence of thermodynamic equilibrium phases in electrolytic aluminium and AlSi12Cu(Fe) alloy were calculated. Then the equilibrium isopleth phase diagram: ver-

tical cross-section through Al-corner with variable contents of Al and Fe (a) and Si (b), and constant contents of all other element was constructed (Figure 5). Graphs show that during solidification in Al-Fe system  $\text{Al}_{13}\text{Fe}$  phase precipitate and in Al-Si system  $\beta\text{-AlFeSi}$  phase precipitate.

Figure 6 a) presents a concentration of iron in dependence from the distance from the iron wire at temperature 750 °C. The dissolution time was 30 min. It also shows the microstructure of interface between iron wire and aluminium, and at the distances 3 mm and 9 mm from the iron wire. In Figure 6 b) the interface between iron wire and aluminium could be seen, and also the needles of iron phases. It is assumed that this is  $\text{Al}_{13}\text{Fe}_4$  phase, formed during peritectic reaction between the electrolytic aluminium and the iron wire. Concentration of iron in aluminium decreased to 0.5 wt.% Fe at distance 3 mm from iron wire.

Figure 7 a) presents a concentration of iron in dependence from distance from iron wire at temperature 750 °C in electrolytic aluminium. The dissolution time was 15 min. Microstructures on distance b) 1 , c) 3 and d) 9 mm from the iron wire are shown on Figure 7. Needles of iron phases are barely visible, interface between iron wire

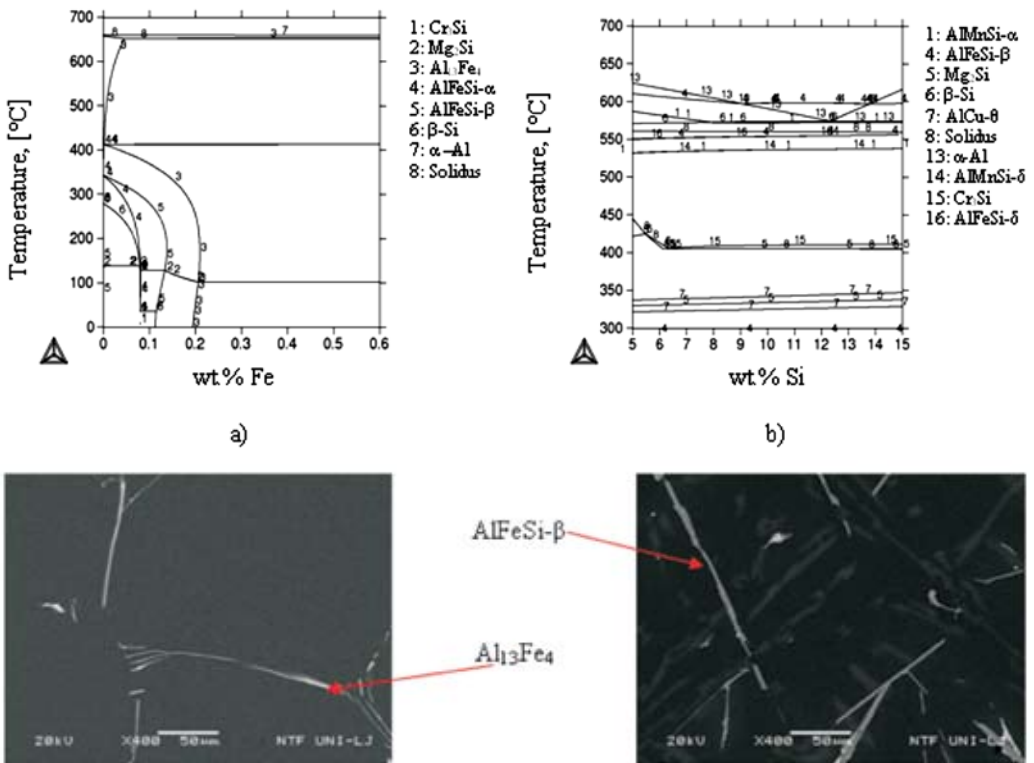


**Figure 5.** Equilibrium isopleth phase diagram of electrolytic aluminium with belonging microstructure of  $\text{Al}_{13}\text{Fe}_4$  phase (a) and  $\text{AlSi12Cu(Fe)}$  alloy with belonging microstructure of  $\text{AlFeSi-}\beta$  phase (b)

**Slika 5.** Ravnotežni izopletni fazni diagram za elektrolizni aluminij s pripadajočimi mikrostrukturnimi fazami  $\text{Al}_{13}\text{Fe}_4$  (a) in zlitino  $\text{AlSi12Cu(Fe)}$  s pripadajočimi mikrostrukturami faze  $\text{AlFeSi-}\beta$  (b)

and aluminium is not shown, concentration of iron in aluminium decreased to 0.8 wt.% at distance 1 mm.

Figure 8 a) presents a concentration of iron in dependence from distance from iron wire at temperature 750 °C in electrolytic aluminium. The dissolution time was 0 min. When the temperature of melt reached 750 °C, the iron wire was placed in the melt and the heating was turned off. On microstructure the interface between iron wire and aluminium is not present and

needles of iron phases are barely visible. Microstructure presents iron phases at the distance 1, 3 in 9 mm from iron wire.

Microstructures were made also on  $\text{AlSi12Cu(Fe)}$  alloy, which is shown by Figures 9-11. Figure 9 a) presents concentration of iron in dependence from distance from iron wire at temperature 750 °C and dissolution time of 30 min in  $\text{AlSi12Cu(Fe)}$  alloy. Shown are also microstructures of interface b) between iron wire and aluminium alloy, and on the

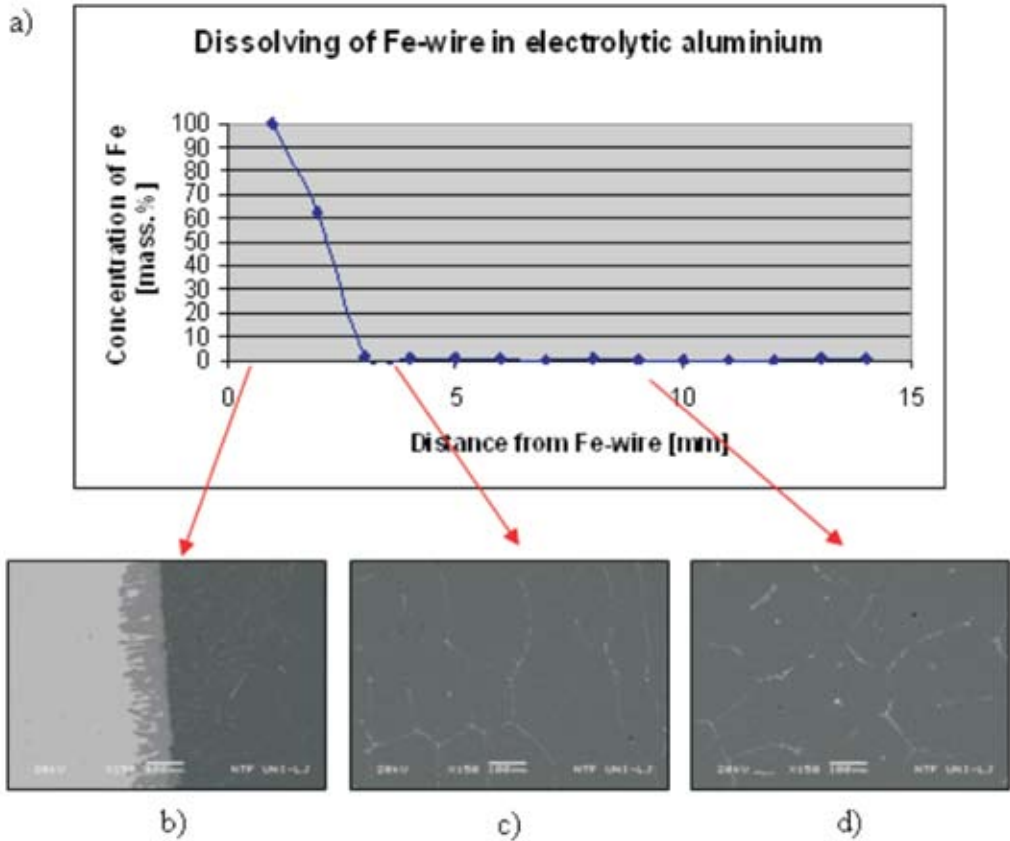


**Figure 6.** a) Concentration of iron in electrolytic aluminium at different distances from the iron wire (the results of EDS analyses). Scanning electron micrographs (BSE) at different distances from the iron wire after 30 min dissolution time at 750 °C: b) at the interface iron wire – electrolytic aluminium, c) 3 mm and d) 9 mm from the interface.

**Slika 6.** a) Koncentracija železa v elektroliznem aluminiju pri različnih razdaljah od železove žičke (rezultati EDS analize). Posnetki elektronskega mikroskopa (odbiti elektroni) pri različnih razdaljah od železove žičke po 30 min raztapljanja pri 750 °C: b) na prehodu železova žička – elektrolizni aluminij, c) 3 mm in d) 9 mm od prehoda.

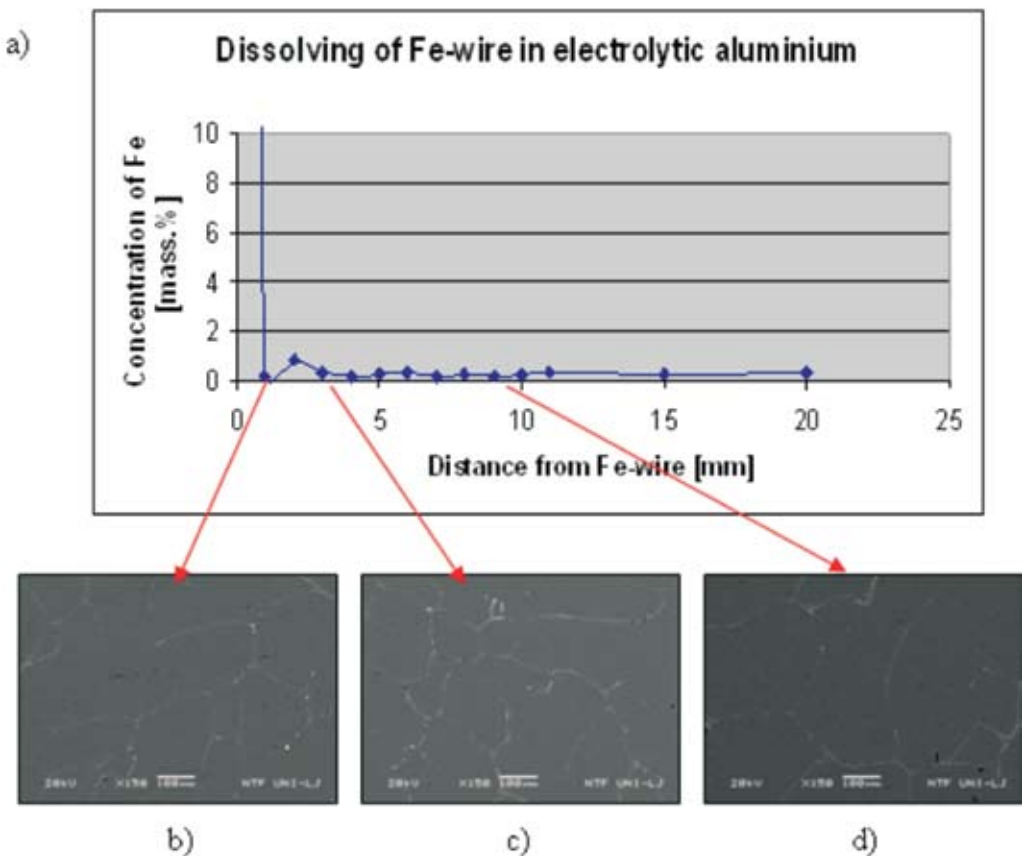


**Figure 7.** a) Concentration of iron in electrolytic aluminium at different distance from iron wire (the results of EDS analyses). Scanning electron micrographs (BSE) at different distances from the iron wire after 15 min dissolution time at 750 °C: b) 1 mm, c) 3 mm and d) 9 mm from the iron wire.

**Slika 7.** a) Koncentracijski železa v elektroliznem aluminiju pri različnih razdaljah od železove žičke (rezultati EDS analize). Posnetki elektronskega mikroskopa (odbiti elektroni) pri različnih razdaljah od železove žičke po 15 min raztapljanja pri 750 °C: b) 1 mm, c) 3 mm in d) 9 mm od železove žičke.



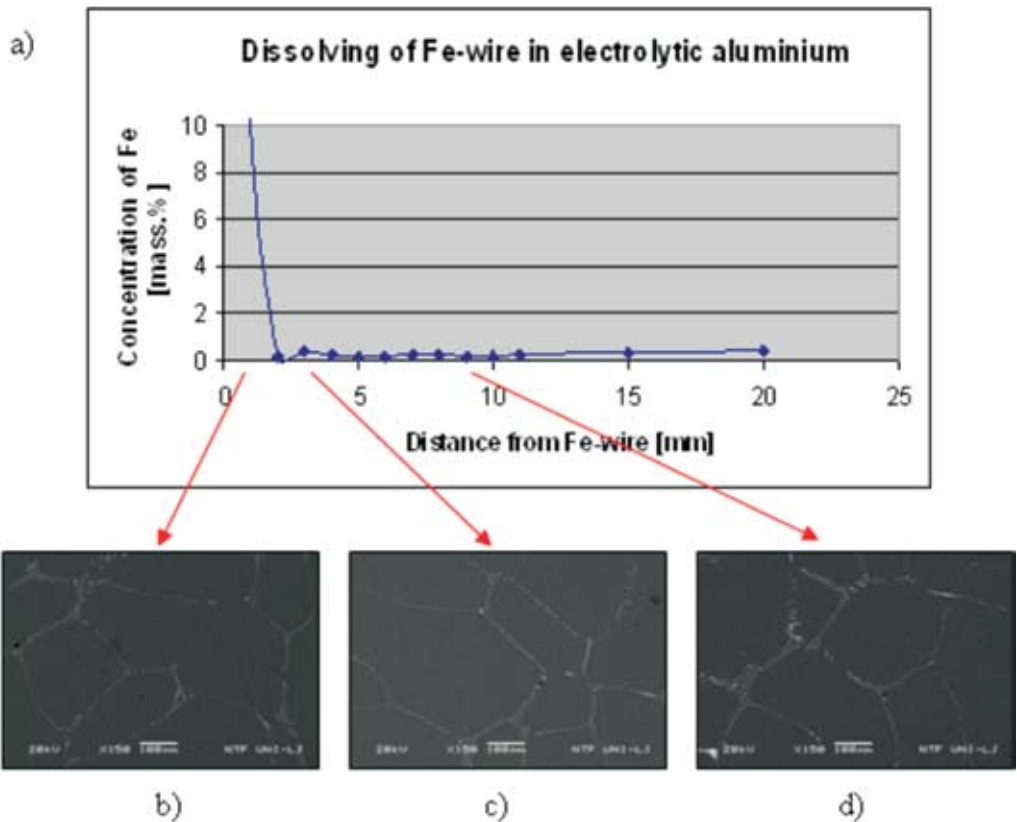


**Figure 8.** a) Concentration of iron in electrolytic aluminium at different distance from iron wire (the results of EDS analyses). Scanning electron micrographs (BSE) at different distances from the iron wire after 0 min dissolution time at 750 °C: b) 1mm, c) 3 mm and d) 9 mm from the iron wire.

**Slika 8.** a) Koncentracijski železa v elektroliznem aluminiju pri različnih razdaljah od železove žičke (rezultati EDS analize). Posnetki elektronskega mikroskopa (odbiti elektroni) pri različnih razdaljah od železove žičke po 0 min raztapljanja pri 750 °C: b) 1mm, c) 3mm in d) 9mm od železove žičke.

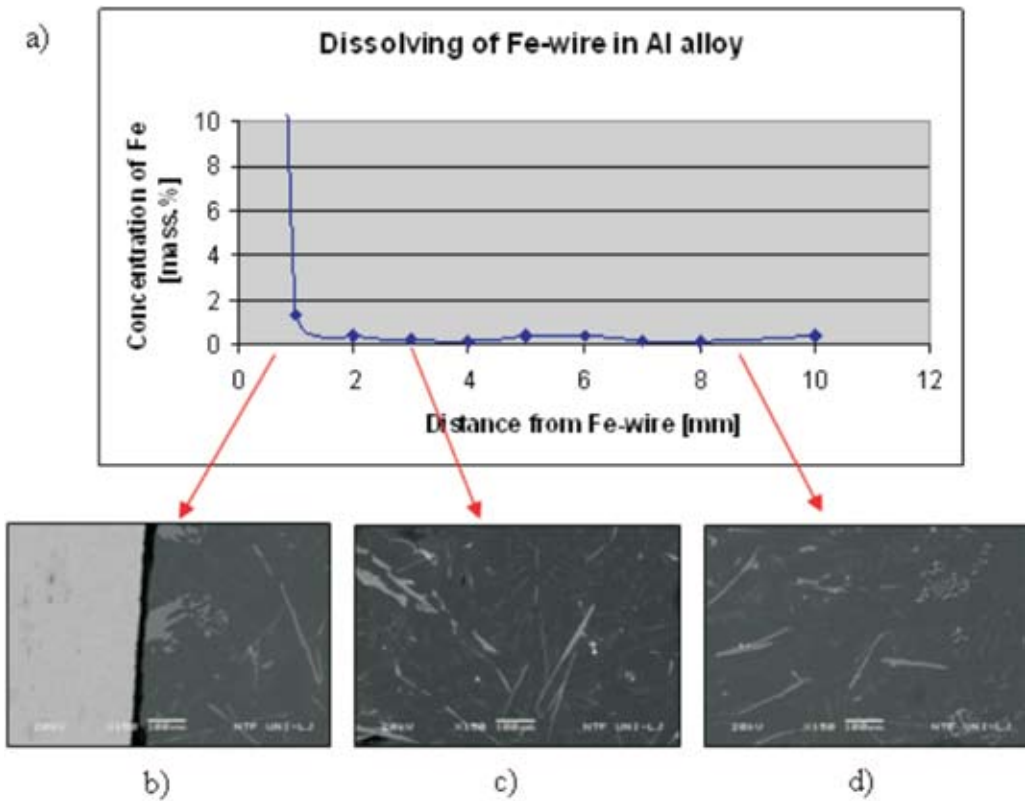


**Figure 9.** a) Concentration of iron in AlSi12Cu(Fe) alloy at different distances from the iron wire (the results of EDS analyses). Scanning electron micrographs (BSE) at different distances from the iron wire after 30 min dissolution time at 750 °C: b) at the interface iron wire – AlSi12Cu(Fe) alloy, c) 3 mm and d) 9mm from the interface.

**Slika 9.** a) Koncentracija železa v zlitini AlSi12Cu(Fe) pri različnih razdaljah od železove žičke (rezultati EDS analize). Posnetki elektronskega mikroskopa (odbiti elektroni) pri različnih razdaljah od železove žičke po 30 min raztapljanja pri 750 °C: b) na prehodu železova žička – zlitina AlSi12Cu(Fe), c) 3 mm in d) 9 mm od prehoda.

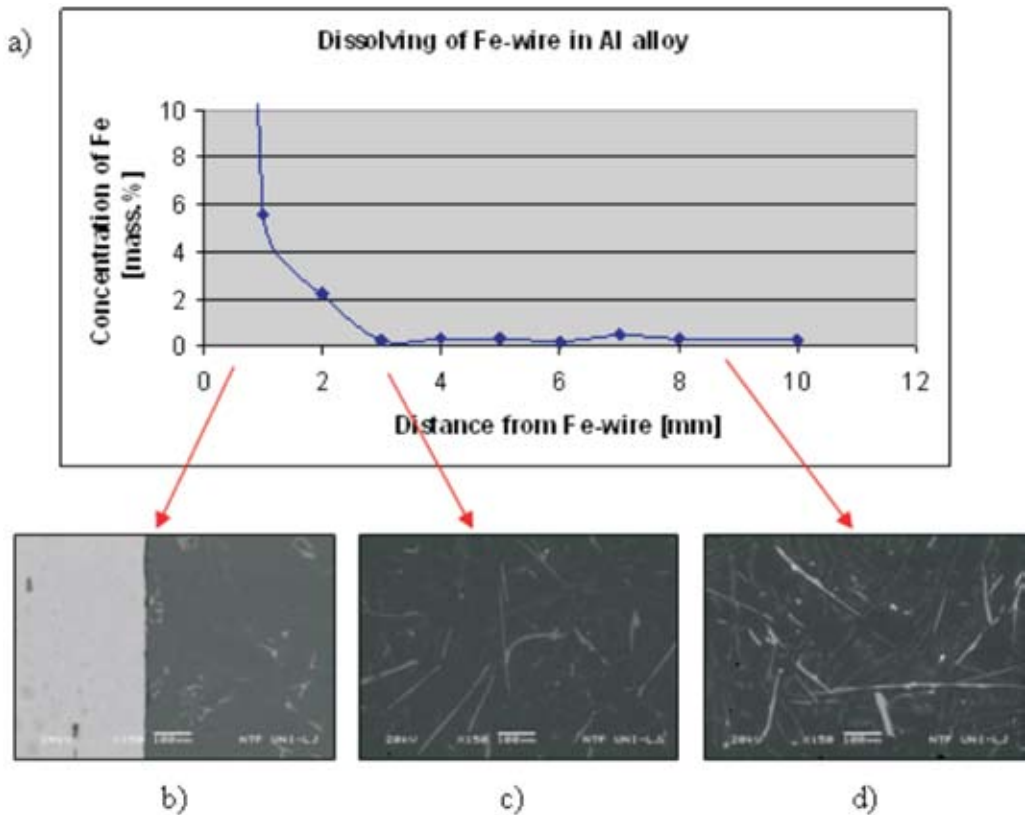


**Figure 10.** a) Concentration of iron in AlSi12Cu(Fe) alloy at different distances from the iron wire (the results of EDS analyses). Scanning electron micrographs (BSE) at different distances from the iron wire after 15 min dissolution time at 750 °C: b) at the interface iron wire – AlSi12Cu(Fe) alloy, c) 3 mm and d) 9 mm from the interface.

**Slika 10.** a) Koncentracija železa v zlitini AlSi12Cu(Fe) pri različnih razdaljah od železove žičke (rezultati EDS analize). Posnetki elektronskega mikroskopa (odbiti elektroni) pri različnih razdaljah od železove žičke po 15 min raztapljanja pri 750 °C: b) na prehodu železova žička – zlitina AlSi12Cu(Fe), c) 3 mm in d) 9 mm od prehoda.

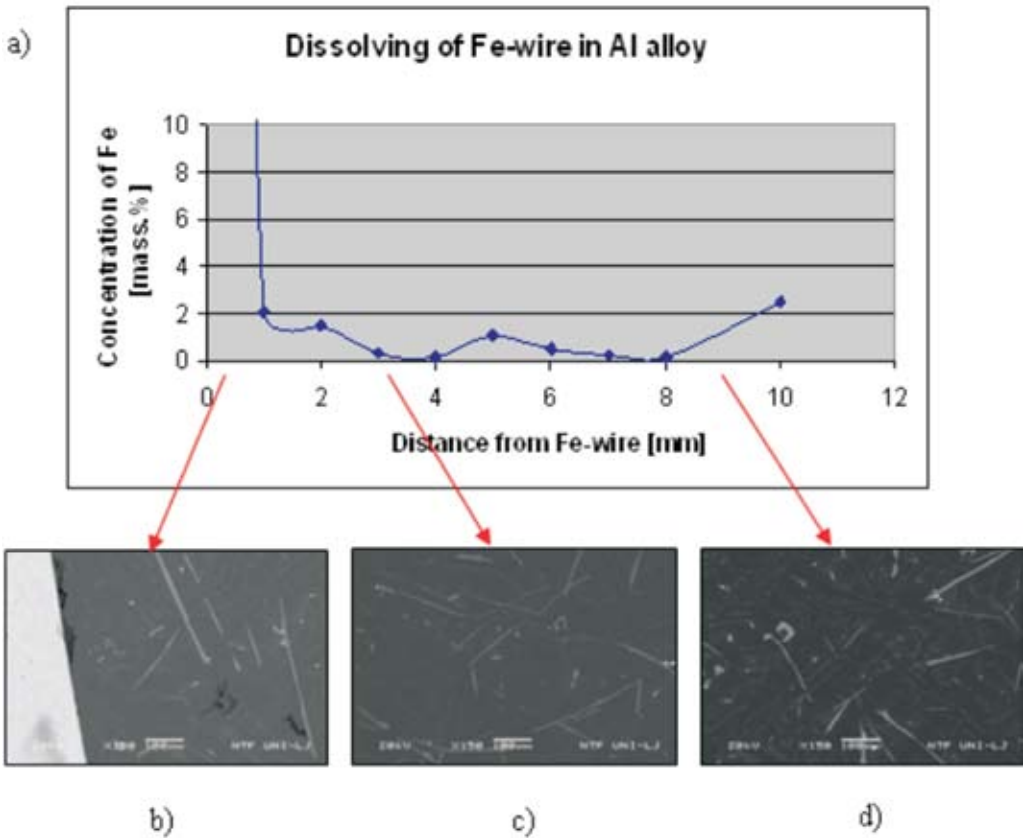


**Figure 11.** a) Concentration of iron in AlSi12Cu(Fe) alloy at different distances from the iron wire (the results of EDS analyses). Scanning electron micrographs (BSE) at different distances from the iron wire after 0 min dissolution time at 750 °C: b) at the interface iron wire – AlSi12Cu(Fe) alloy, c) 3 mm and d) 9 mm from the interface.

**Slika 11.** a) Koncentracija železa v zlitini AlSi12Cu(Fe) pri različnih razdaljah od železove žičke (rezultati EDS analize). Posnetki elektronskega mikroskopa (odbiti elektroni) pri različnih razdaljah od železove žičke po 0 min raztapljanja pri 750 °C: b) na prehodu železova žička – zlitina AlSi12Cu(Fe), c) 3 mm in d) 9 mm od prehoda.

distance 3mm c) and 9 mm d) from iron wire. Dissolving iron combines with Al and Si and forms  $\beta$ -AlFeSi phase. Interface between iron wire and aluminium alloys is not present as by electrolytic aluminium. Concentration of iron in aluminium alloy decreased to 0.3 wt.% at the distance 1 mm from iron wire.

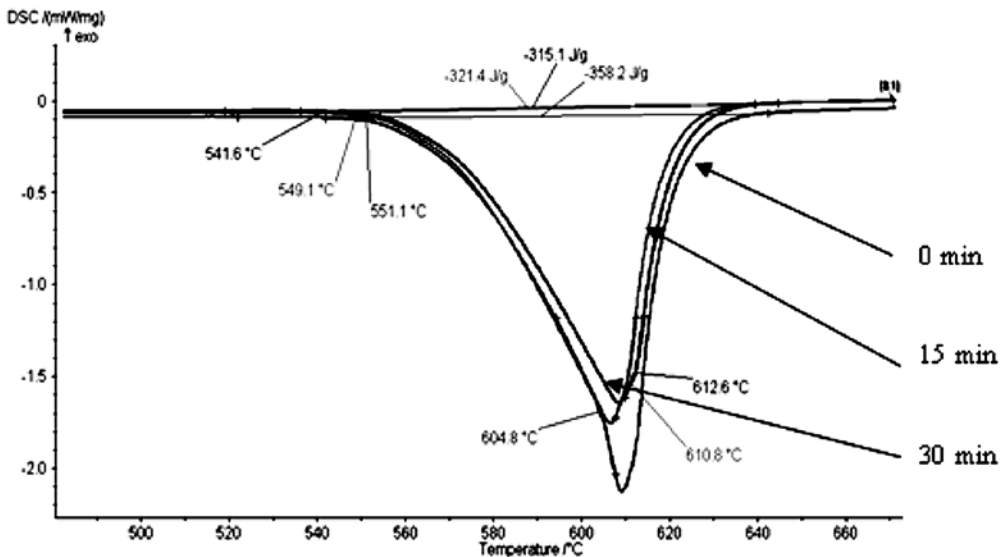
Figure 10 presents concentration of iron in dependence from distance from iron wire at temperature 750 °C and dissolution time of 15 min in AlSi12Cu(Fe) alloy. Shown are also microstructures of interface between iron wire and aluminium alloy, and at the distance 3 mm and 9 mm from iron wire. Interface between iron wire and aluminium alloys, and needles from iron wire are not visible. Concentration of iron in aluminium alloy decreased to 0.2 wt.% at distance 3 mm from iron wire.

Figure 11 presents concentration of iron in dependence from distance from iron wire in AlSi12Cu(Fe) alloy and dissolution time of 0 min, which was heated up to 750 °C. Shown are also microstructures of interface between iron wire and aluminium alloy, and on the distance of 3 mm and 9 mm from iron wire. When the temperature of the melt reached 750 °C, the iron wire was placed into the melt and the heating was turned off. Interface between iron wire and aluminium alloy is seen on microstructures. The concentration of iron in alloy varies between 0.2 and 2 wt.% of iron.

For samples of AlSi12Cu(Fe) alloy with iron wires was made simultaneous thermal analysis. Figure 12 and 13 presents comparison between heating curves of investigated AlSi12Cu(Fe) alloy and heat of fusion. Notice that with increasing dissolution time of iron wire in melt at 750 °C, the liquidus temperature decreased and eutectic temperature increased. This can be a consequence of increasing iron concentration in the alloy. Comparison of solidus temperatures and their heats of fusion is presented in Table 3.

With the simultaneous thermal analysis were measured temperatures of precipitation and the heats of fusion. From diagram on Figures 6 is shown that at specified temperature AlCu- $\theta$  is precipitated. The curves in Figure 14 can show that increasing dissolution time of iron wire in the melt at 750 °C, the precipitation temperature and therefore heats of fusion decreased. Comparison of precipitation temperatures and heats of fusion are presented in Table 4.

Figure 15 compares cooling curves after different dissolution times of iron wire in AlSi12Cu(Fe) alloy. The curves show that the temperature of primary solidification and temperature of eutectic solidification are similar. The longer is the dissolution time of the iron wire in the melt at 750 °C, less heat is released during solidification. Table 5 shows temperatures of primary solidification, eutectic solidification and heats of fusion.



**Figure 12.** Comparison of heating curves of investigated samples in the AlSi12Cu(Fe) alloy

**Slika 12.** Primerjava segrevalnih krivulj preiskovanih vzorcev v zlitini AlSi12Cu(Fe)

**Table 3.** Comparison of melting temperatures and their heats of fusion

**Tabela 3.** Primerjava temperatur začetka taljenja in latentnih toplot, ki se porabijo pri taljenju

DISSOLUTION TIME	0 MIN	15 MIN	30 MIN
$T_{\text{solidus}}$	551.1 °C	549.1 °C	541.6 °C
$T_{\text{eutectic}}$	604.8 °C	610.8 °C	612.6 °C
Heat of fusion	358.2 J/g	321.4 J/g	315.1 J/g

**Table 4.** Segregation temperatures for AlCu- $\theta$  phase and their latent heats after different dissolution times of iron wire in AlSi12Cu(Fe) alloy

**Tabela 4.** Primerjava temperatur izločanja za fazo AlCu- $\theta$  in njihovih latentnih toplot po različnih časih raztapljanja železove žičke v zlitini AlSi12Cu(Fe)

DISSOLUTION TIME	0 MIN	15 MIN	30 MIN
$T_{\text{segregation}}$	261.4 °C	235.5 °C	237.5 °C
Precipitation heat	8.739 J/g	6.337 J/g	5.737 J/g

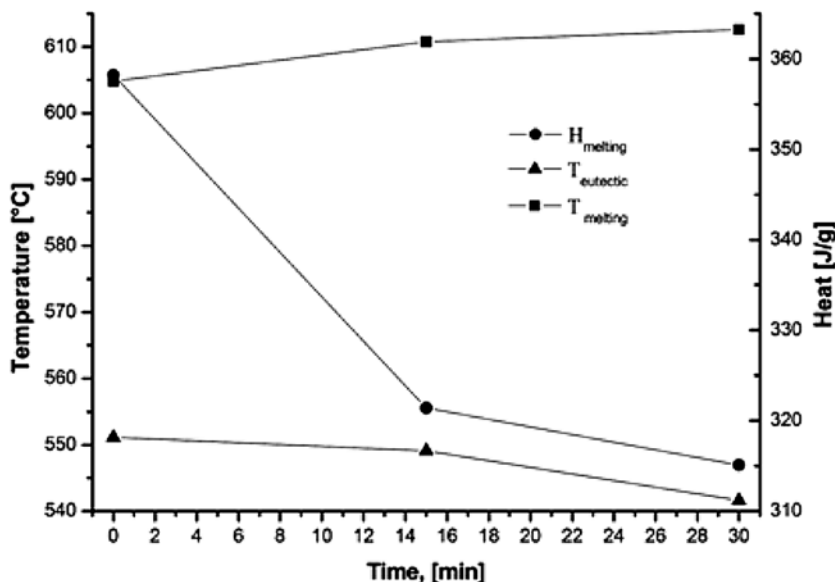


**Figure 13.** Melting temperatures and heats of fusion depending on dissolution time of iron wire in AlSi12Cu(Fe)

**Slika 13.** Temperatura taljenja in porabljena latentna toplota v odvisnosti od časa raztapljanja Fe-žičke v zlitini AlSi12Cu(Fe)

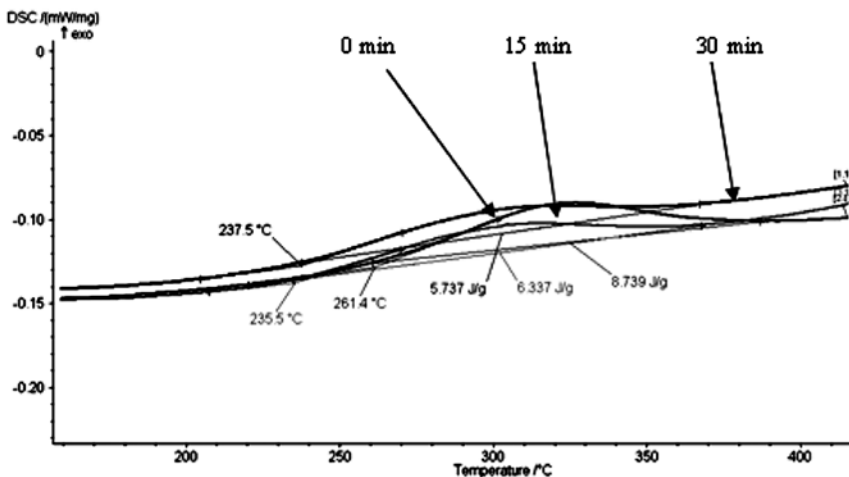


**Figure 14.** Comparison of cooling curves after different dissolution times of iron wire in AlSi12Cu(Fe) alloy in the temperature region, where precipitation of AlCu- $\theta$  phase is expected. The latent heats of precipitation are also given.

**Slika 14.** Primerjava ohlajevalnih krivulj po različnih časih raztapljanja železove žičke v zlitini AlSi12Cu(Fe) v temperaturnem območju, kjer se pričakuje izločanje faze AlCu- $\theta$ . Podane se tudi latentne toplote izločanja.

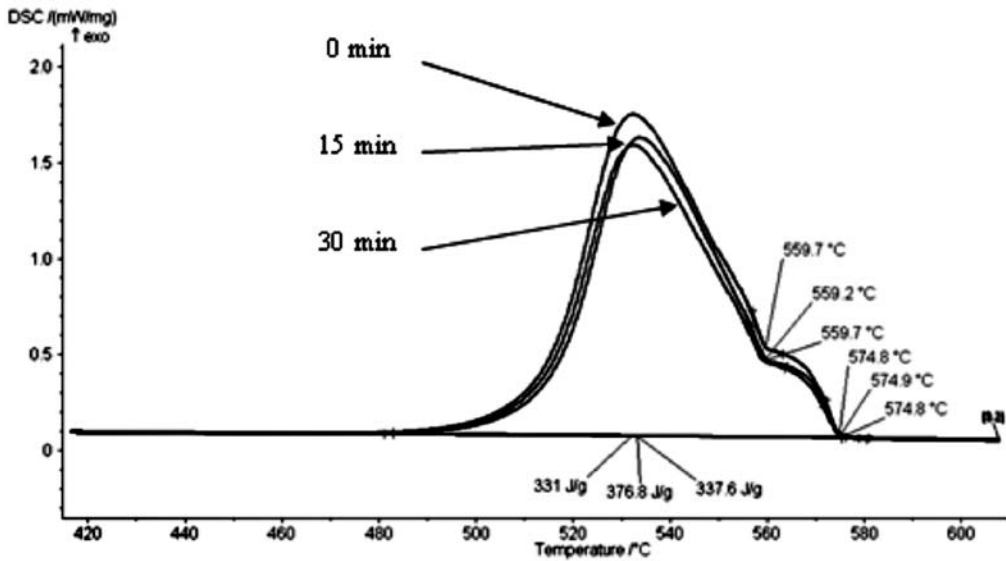


**Figure 15.** Cooling curves after different dissolution times of iron wire in AlSi12Cu(Fe) alloy and corresponding heats of fusion (solidification)

**Slika 15.** Ohlajevalne krivulje po različnih časih raztapljanja železove žičke v zlitini AlSi12Cu(Fe) ter pripadajoče latentne toplote

**Table 5.** Temperatures of primary solidification, eutectic solidification and heats of fusion (solidification) after different dissolution times of iron wire in AlSi12Cu(Fe) melt

**Tabela 5.** Temperature začetka strjevanja, strjevanja evtektika in latentnih toplot, po različnih časih raztapljanja železove žičke v talini zlitine AlSi12Cu(Fe)

DISSOLUTION TIME	0 MIN	15 MIN	30 MIN
$T_{\text{liquidus}}$	574.9 °C	574.8 °C	574.8 °C
$T_{\text{eutectic}}$	559.7 °C	559.7 °C	559.2 °C
Heat of fusion	376.8 J/g	337.6 J/g	331 J/g



## CONCLUSIONS

The purpose of experiments was to determine of iron dissolution in electrolytic aluminium and in AlSi12Cu(Fe) alloy. According to the results the following conclusions can be drawn:

- In Al-Fe system most often iron phase  $Al_{13}Fe_4$  is present. In AlSi12Cu(Fe) alloy  $\beta$ -AlFeSi phase crystallized as a primary phase, in which most of the iron from Fe-wire is present.
- The highest concentration of iron in electrolytic aluminium is obtained after dissolution iron wire for 30 min at 750 °C. Iron concentration diagram becomes apparently constant 4 mm from Fe-wire, when the content of Fe in aluminium decreased to 0.5 wt.% Fe.
- Concentration profile of dissolving iron in Al-Si alloy is different probably due to binding of iron from iron wire in the primary solidified  $\beta$ -AlFeSi phase. Concentration of Fe in AlSi12Cu(Fe) alloy drops to 0.3 wt.% Fe at distance 1 mm from iron wire after 30 min dissolution time at 750 °C.
- With the help of simultaneous thermal analysis we can claim that by increasing concentration of iron in alloy the solidus temperature decreased and eutectic temperature increased.
- By increasing the concentration of iron the latent heat for melting (heat of fusion) decreased. Iron phases released less heat during solidification, which was proven by simultaneous thermal analysis.

- By increasing concentration of iron in alloy the temperature for precipitation of AlCu- $\theta$  phase and amount of released latent heat were decreased.

## POVZETEK

### Raztapljanje železa v aluminijevih zlitinah

Železo predstavlja v aluminijevih zlitinah glavno nečistočo. Pri nekaterih aluminijevih zlitinah pa je glavni zlitinski element, ki izboljša trdoto zlitine, vendar s tem poveča krhkost. V tem delu smo preiskovali kako se železo raztaplja v elektroliznem aluminiju in zlitini AlSi12Cu(Fe). Raztapljanje železa smo preiskovali z vstavljanjem Fe-žičke v elektrolizni aluminij in zlitino AlSi12Cu(Fe), pri temperaturi 750 °C in različnih časih raztapljanja: 0, 15 in 30 minut. Ko je talina dosegla temperaturo 750 °C, smo vanj vstavili železovo žičko in jo pri tej temperaturi držali v talini različno dolgo. Nato smo vzorce razrezali tik ob žički in jih preiskali z vrstičnim elektronskim mikroskopom (SEM), kjer smo ugotavljali koncentracijo Fe v aluminiju in aluminijevi zlitini ter katere železove faze se izločajo. Z računalniško simulacijo Thermo-Calc smo ugotovili, da se v sistemu Al-Fe pri strjevanju elektroliznega aluminija izloča faza  $Al_{13}Fe_4$  pri zlitini AlSi12Cu(Fe) pa faza AlFeSi- $\beta$ . Z elektronskim mikroskopom smo analizirali železovo žičko, in vsak milimeter vstran od železove žičke ter naredili posnetek. Nato smo izdelali koncentracijski diagram koncentracije železa v odvisnosti od oddaljenosti žičke.

S simultano termično analizo (STA) smo določali karakteristične temperature in toplote taljenja, strjevanja in izločanja. Opazili smo, da dlje kot smo držali Fe-žičko pri 750 °C, nižje so likvidus temperature in višje so temperature taljenja evtektika, kar je posledica povečanja deleža železa v zlitini. Prav tako lahko rečemo, da dlje ko smo žičko držali pri temperaturi 750 °C, nižjo temperaturo izločanja faze AlCu- $\theta$  smo dobili in s tem tudi nižje toplote. Iz ohlajevalnih krivulj simultane termične analize pa je razvidno, da dlje kot smo Fe-žičko držali na temperaturi 750 °C v talini, manj toplote se sprosti pri strjevanju.

Najpogostejša faza, ki se pojavlja v sistemu aluminij-železo je faza Al<sub>13</sub>Fe<sub>4</sub>. V Al-Si zlitinah lahko srečamo številne železove intermetalne spojine, kar je odvisno od kemijske sestave in pogojev strjevanja. Najpogostejše primarno izločene faze so  $\alpha$ -Al<sub>8</sub>Fe<sub>2</sub>Si,  $\beta$ -Al<sub>5</sub>FeSi in  $\delta$ -Al<sub>9</sub>FeSi<sub>2</sub>. V zlitini AlSi12Cu(Fe) je bila primarno izločena faza  $\beta$ -AlFeSi, na katero se je nalagalo tudi železo od raztapljanja Fe-žičke. Najvišjo koncentracijo železa aluminiju smo dobili z raztapljanjem žičke pri 750 °C in času 30 min. Krivulja koncentracijskega diagrama se izravna nekje na oddaljenosti 4 mm od žičke, vsebnost Fe v aluminiju pa pade na 0,5 mas.% Fe. Pri aluminijevi zlitini pa vsebnost železa v aluminijevi zlitini pade že na 1 mm od žičke na 0,3 mas. %, pri raztapljanju žičke na 750 °C 30 min. Z večanjem deleža železa v zlitini se znižuje temperatura tališča, temperatura tališča evtektika pa se zvišuje. Z večanjem deleža železa v zlitini se zniža tudi toplota, ki se porablja pri taljenju. Prav tako lahko rečemo, da železove faze oddajo manj toplote pri strjevanju, kar je razvidno tudi iz preiskav s simultano termično analizo.

## REFERENCES

- [1] BELOV, N.A., AKSENOV, A.A., ESKIN, D.G. (2002): *Iron in Aluminum Alloys: Impurity and Alloying Element*. London and New York, pp. 3-7.
- [2] MARKOLI, B., SPAIČ, S., ZUPANIČ, F. (2004): The intermetallic phases containing transition elements in common Al-Si cast alloys. *Aluminium*; Vol. 80, No. 1/2, pp. 84-88.
- [3] MASSALSKI, T.B. (1990): *Binary Alloys Phase Diagrams*. 2<sup>nd</sup> ed., ASM, Metals Park, Ohio.